First-principles predictions of potential hydrogen storage materials: Nanosized Ti(core)/Mg(shell) hydrides

S. X. Tao, P. H. L. Notten, R. A. van Santen, and A. P. J. Jansen
Eindhoven University of Technology, Laboratory of Inorganic Chemistry and Catalysis, P. O. Box 513, NL-5600 MB, Eindhoven, The Netherlands

(Received 3 February 2011; revised manuscript received 30 March 2011; published 3 May 2011)

MgH_2 is one of the most promising hydrogen storage materials. However MgH_2 is thermodynamicly too stable, leading to a too high desorption temperature of 300 °C at atmospheric pressure, which is a major impediment for practical applications. In this study, aiming to tune the thermodynamic stability of the MgH_2, nanosized two-dimensional Mg/Ti/Mg sandwich and three-dimensional Ti(core)/Mg(shell) hydrides have been investigated by using density functional theory calculations. For both structures, four types of hydrogen atoms can be distinguished: on the surface of the Mg (H_{surf}), within the Mg (H_{Mg}), at the Mg/Ti interface (H_{MgTi}), and within the Ti (H_{Ti}). For the dehydrogenation reaction, the hydrogen desorption from the hydride is in the order H_{surf}, H_{Mg}, H_{MgTi}, H_{Ti}. The desorption energy of H_{surf} is unexpectedly high. As expected, due to the well-preserved fluorite structure of the partially hydrogenated hydride, the desorption energy of H_{Mg} is significantly lower than that of bulk rutile MgH_2. The further desorption of H_{MgTi} and H_{Ti} becomes more difficult due to the strong Ti-H bonding. We propose that partial hydrogenation without adsorption of H_{surf} and partial dehydrogenation without desorption of H_{MgTi} and H_{Ti} would keep the fluorite symmetry with its favorable thermodynamics. The reversible hydrogen capacity (H_{Mg}) of the Mg/Ti/Mg sandwich structure is low, whereas the reversible hydrogen capacity of the Ti(core)/Mg(shell) is calculated to be reasonable high. Our results predicted Ti(core)/Mg(shell) structures are potential useful materials for hydrogen storage application.

DOI: 10.1103/PhysRevB.83.195403 PACS number(s): 88.30.R−, 68.35.Md, 68.65.Ac

I. INTRODUCTION

MgH_2 is one of the most attractive hydrogen storage materials because it is inexpensive and light.[1–3] However, the kinetics of the hydrogen uptake and release in Mg is poor. It is generally accepted that the diffusion limitations, high oxidation sensitivity of the Mg surface, and high activation barrier of hydrogen molecule dissociation leads to poor hydrogen kinetics in Mg. Another disadvantage of MgH_2 is too stable, leading to too high desorption temperatures (T_d) at atmospheric pressure. For example, the desorption energy of MgH_2 is 75 kJ/mol H_2, i.e., 0.78 eV/H_2 (T_d = 300 °C),[4] while a desorption energy of 20–50 kJ/mol H_2, i.e., 0.21–0.52 eV/H_2 (T_d = 20–100 °C) is desirable. Tuning kinetics of MgH_2 has been achieved by means of alloying Mg with transition metals (TMs), adding catalyst and mechanical ball milling.[5–28] Among the Mg-TM-H hydrides, Mg-Ti-H is one of the most widely investigated systems because of its tremendous potential for improving the (de)hydrogenation kinetics.[18–21] The fcc symmetry of the Mg-Ti-H system has been claimed to be responsible for the improved kinetics.[19–21] The structural transformation from rutile to fluorite in Mg-Ti-H has been theoretically confirmed for both bulk[29,30] and multilayered systems.[31]

Besides the improved kinetics, tuning of the thermodynamics of Mg-Ti-H has been reported for various morphologies, i.e., nanostructured particles,[26] thin films,[27] and multilayers.[28] Nanostructured Mg-Ti-H by mixing MgH_2 and TiH_2 and ultrahigh energy high-pressure mechanical milling has been prepared by Lu *et al.*[26] Their results show that the dehydrogenation energy of MgH_2-0.1TiH_2 is lower than that of MgH_2. For the rehydrogenation of the dehydrogenated alloys, fast hydrogen absorption was also observed at room temperature. Baldi *et al.*[27,28] managed to tune the thermodynamics of hydrogen absorption in the Mg-Ti-Pd system by means of elastic clamping. Their results show that the thermodynamics of hydrogen absorption in Pd-capped Mg films are strongly dependent on the Mg thickness.[27] Furthermore, Mg/Ti multilayers with various monolayer thicknesses between 0.5 and 20 nm were prepared. The layer thickness dependence of the hydrogenation properties was reported. Besides the elastic clamping effect of the Pd layer, the interface effect was also proposed to be responsible for the different thermodynamics.[28]

Despite all the experimental progress, the origin of the tuned thermodynamics of Mg-H bonding is still not well understood. Theoretical studies[32–37] have reported that using nanoparticles instead of bulk or coarse particles of hydrides can alter the thermodynamics of hydrogen uptake and release. Because the energies of both metals and hydrides change going from bulk materials to nanosized particles, the reaction thermodynamics will be affected by the size of the grains. Moreover, our previous theoretical study has shown that the structural transformation of MgH_2 from rutile to fluorite induced by contacting with a TM plays an important role in tuning the thermodynamics in the MgH_2/TMH_2 multilayers.[31] In MgH_2/TMH_2 multilayers, notable destabilization of Mg-H bonding could be observed with a high Ti:Mg ratio and very thin Mg layers (a few nanometers). This, however, leads to a significant reduction of the reversible hydrogen storage capacity due to the fact that parts of the hydrogen atoms are trapped in the TM. Stimulated by the promising results reported above, we consider combining the destabilized Mg-H bondings in the fluorite structure by alloying with Ti, and the surface effect in the nanosized materials. We propose that by extending the two-dimensional (2D) structure to three

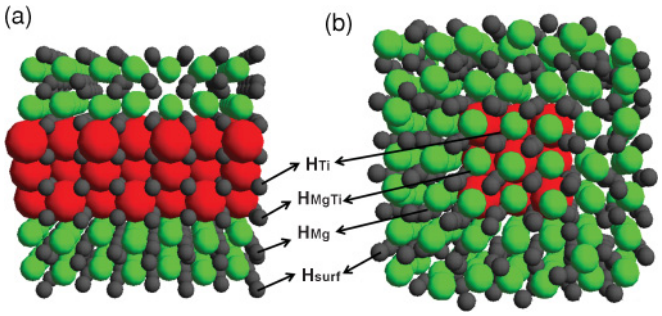

FIG. 1. (Color online) Four types of hydrogen atoms in (a) 2D Mg/Ti/Mg sandwich structure and (b) 3D Ti(core)/Mg(shell) structure. The red (large), green (medium), and dark gray (small) spheres represent Ti, Mg, and hydrogen atoms, respectively. The same colors (scheme) are applied in the following figures.

dimensions (3D), the kinetics and thermodynamics can be improved and that a larger reversible hydrogen storage capacity can be expected. To verify this hypothesis, 2D Mg/Ti/Mg sandwich and 3D Ti(core)/Mg(shell) structures have been designed and studied by large-scale density functional theory (DFT) calculations. We intend to give a prediction of the thermodynamic properties in such nanostructured materials, thus helping to design unique hydrogen storage materials.

II. STRUCTURAL MODELS AND COMPUTATIONAL METHODS

Figure 1 shows the models for the Mg/Ti/Mg sandwich and Ti(core)/Mg(shell) structures. For simplicity, the 2D slab is cut from fluorite hydride with a (100) plane and the 3D particle is cut from fluorite hydride with a cubic symmetry. Four types of hydrogen atoms can be recognized in both structures: hydrogen on the surface of the Mg (H_{surf}), within the Mg (H_{Mg}), at the Mg/Ti interface (H_{MgTi}), and within the Ti (H_{Ti}). Three different sizes of the 2D (Fig. 2) and 3D (Fig. 3) structures are constructed by putting one, two, or three atomic layers of Mg on a fixed-sized Ti slab or Ti core.

All calculations were performed using DFT as implemented in the Vienna *Ab Initio* Simulation Package (VASP).[38,39] The Kohn-Sham equations were solved using a basis of plane-wave functions with a plane-wave energy cutoff of 400 eV,[40] and using pseudopotentials[41] to describe the core electrons. The Perdew-Wang 1991 generalized gradient approximation was used for the electron-exchange correlation potential.[42] For the 2D Mg/Ti/Mg sandwich structure (Fig. 2), (2×2) supercells were always used. A total of $7 \times 7 \times 1$ k points were used to model the Brillouin zone. For the 3D Ti(core)/Mg(shell) structures, k-space integration is restricted to the Γ point only. Since periodic boundary conditions are involved, the size of the supercell containing the 2D nanoslab and 3D nanoparticle was chosen such that the distance between atoms of the periodic images exceeded 15 Å. This was sufficient to avoid interaction of the cluster with its images. Therefore, the calculations of $Ti_{14}Mg_{48}$, $Ti_{14}Mg_{158}$, and $Ti_{14}Mg_{350}$ (shown in Fig. 3) have been proformed using a cubic supercell with sizes of $22 \times 22 \times 22$, $30 \times 30 \times 30$, and $38 \times 38 \times 38$ Å^3, respectively. For all structures, the lattice parameters, the volume, and the atom positions were allowed to relax.

III. RESULTS AND DISCUSSIONS

This section is divided into two parts. In the first part, the Mg/Ti/Mg sandwich structure is studied. The absorption sites and concentration of H_{surf} and the absorption and desorption sequences of the four types of hydrogen atoms are investigated. After that, the size dependence of the dehydrogenation energies is studied. In the second part, extending the 2D structure to a 3D one, the Ti(core)/Mg(shell) structure is studied in a similar manner to the sandwich structure. We focus on the tuned thermodynamics, in particular, the relations between the thermodynamics and the structures and the Ti:Mg ratios. Furthermore, an oversaturation of the Ti(core)/Mg(shell) structure with extra H_{surf} is studied by electronic and geometric structure calculations. Finally, the reversible capacities are determined and compared to the 2D structure.

A. Mg/Ti/Mg sandwich structure

1. H_{surf}

Figure 4 displays the top view of the optimized Mg/Ti/Mg sandwich structure with five different distributions of H_{surf}. After optimization, the hydrogen molecules in structure (a) and (b) have been "pushed" out from the Mg surfaces. The optimized Mg-H_2 distances are 3.79 and 3.76 Å for (a) and (b), respectively. The desorption energies of these hydrogen molecules are nearly zero. This indicates that molecular hydrogen does not form chemical bonds with the Mg surface. For atomic hydrogen with a concentration of H/M = 2 shown in (c), half of the hydrogen atoms have associated to molecular hydrogen after optimization. These hydrogen molecules are far away from the Mg surface with a distance of ~3.50 Å. The remaining half of the hydrogen atoms are located closely to the Mg surface at short bridge sites. The optimized structures of (d) and (e) both demonstrate that short bridge sites with a concentration of H/M = 1 is the most stable structure. Altogether, considering two Mg surfaces per 2D slab, a hydrogen concentration of H/M = 2 for the whole system can be obtained. Therefore, the possibility of the oversaturated hydride can be excluded.

2. Hydrogen absorption and desorption sequences

To study the different thermodynamic properties for the four types of hydrogen atoms, hydrogen absorption and desorption energies in the Mg/Ti/Mg sandwich structure [$Ti_{24}Mg_{32}H_x$ in Fig. 2(b)] have been calculated according to the following equations,

$$\Delta E_{H_{absorption}} = E_{Mg_xTi_{1-x}H_{y+z}} - E_{Mg_xTi_{1-x}H_y} - \frac{z}{2}E_{H_2}, \quad (1)$$

$$\Delta E_{H_{desorption}} = E_{Mg_xTi_{1-x}H_y} + \frac{z}{2}E_{H_2} - E_{Mg_xTi_{1-x}H_{y+z}}, \quad (2)$$

where $E_{Mg_xTi_{1-x}H_y}$ and $E_{Mg_xTi_{1-x}H_{y+z}}$ are the total energy of $Mg_xTi_{1-x}H_y$ and $Mg_xTi_{1-x}H_{y+z}$ normalized to the number of metal atoms.

The hydrogen absorption and desorption sequences are determined by comparing the hydrogen absorption and desorption energies at different hydrogen locations. The calculated energies are summarized in Table I. For instance,

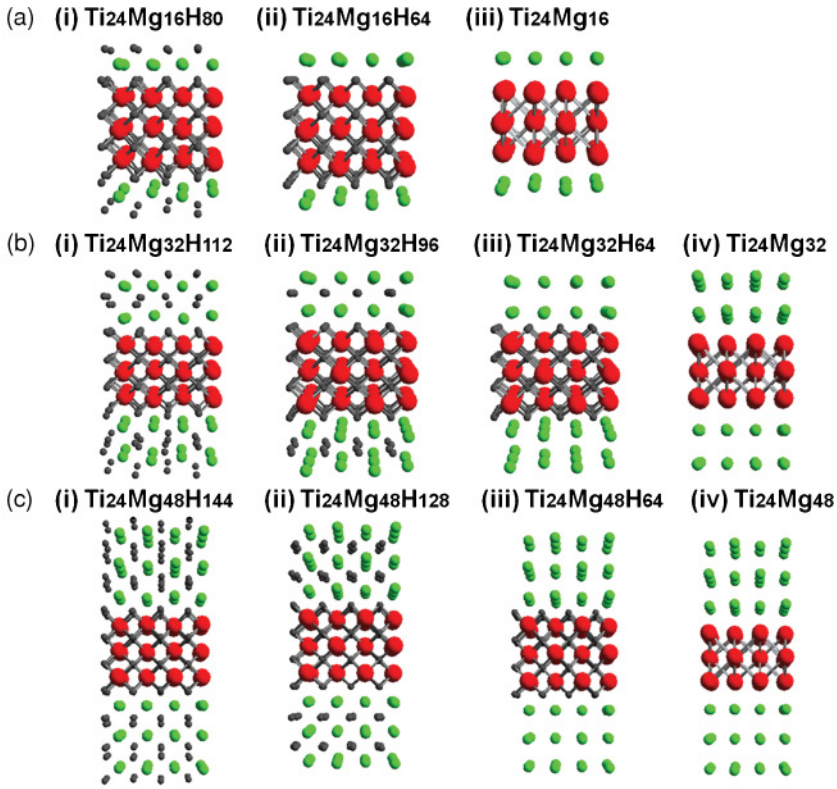

FIG. 2. (Color online) Optimized 2D Mg/Ti/Mg sandwich alloys and their fully and partially hydrogenated hydrides involved in the (de)hydrogenation processes. For each Ti/Mg composition, the structures from the left-hand side to the right-hand side indicate the dehydrogenation process.

$Ti_{24}Mg_{32}H_{112-16}$ denotes that 16 hydrogen atoms are removed from each type of hydrogen location in the $Ti_{24}Mg_{32}H_{112}$. Four types of hydrogen are considered and the desorption energy of H_{surf} is the lowest, therefore H_{surf} will desorb first. After the desorption of H_{surf}, $Ti_{24}Mg_{32}H_{96-32}$ denotes desorption of 32 hydrogen atoms of H_{Mg}, H_{MgTi}, or H_{Ti} from $Ti_{24}Mg_{32}H_{96}$. The desorption energy of H_{Mg} is the lowest, therefore it will desorb secondly. When there are only H_{MgTi} and H_{Ti} left, H_{MgTi} will desorb before H_{Ti}. Therefore, for the dehydrogenation reaction, the desorption of hydrogen follows the order of H_{surf}, H_{Mg}, H_{MgTi}, and H_{Ti}. For the stepwise dehydrogenation energies are 1.15 eV/H_2 for H_{surf}, 0.38 eV/H_2 for H_{Mg}, 1.30 eV/H_2 for H_{MgTi}, and 1.10 eV/H_2 for H_{Ti}. The desorption energy of H_{surf} is surprisingly high. They are many higher than the hydrogen desorption energy in bulk MgH_2 (0.65 eV/H_2).[31] After the desorption of H_{surf}, the desorption of H_{Mg} becomes much easier with very low desorption energy. As expected, after the desorption of H_{surf} and H_{Mg}, the desorption of H_{MgTi} and H_{Ti} becomes more difficult due to the introduction of strong Ti-H bonding. The absorption sequence was determined in a similar manner: The location with the lowest absorption energy (H_{Ti}) absorbs hydrogen first; after the absorption of the H_{Ti}, the absorption of the H_{MgTi} is the most favorable in the remaining three. The absorption sequence is calculated to be the opposite to the desorption sequence: H_{Ti}, H_{MgTi}, H_{Mg}, H_{surf}.

3. *The size dependence of the dehydrogenation energies*

The different thermodynamic properties of the four types of hydrogen species predicted above indicates the potential to tune the thermodynamics of dehydrogenation reaction of the 2D Mg/Ti/Mg sandwich structure. In particular, the populations of different types of hydrogen depend highly on the size and composition of the structure. Average and stepwise dehydrogenation energies of the $Ti_{24}Mg_{16}H_{80}$ [Fig. 2(a)] and $Ti_{24}Mg_{48}H_{144}$ [Fig. 2(c)] have been calculated and compared to those of the $Ti_{24}Mg_{32}H_{112}$ [Fig. 2(b)] studied in Sec. III A 2. The calculated hydrogen desorption sequence of H_{surf}, H_{Mg}, H_{MgTi}, and H_{Ti} in Sec. III A 2 were applied.

As one can see in Table II, the dehydrogenation energies of all the three structures with the desorption of H_{surf} are surprisingly high. The reason will be explained further with the structural analyses in Sec. III B 2. Similar to that of $Ti_{24}Mg_{32}H_{112}$, the desorption of H_{Mg} for $Ti_{24}Mg_{32}H_{112}$

TABLE I. Hydrogen desorption and absorption energies (in eV/H_2).

Desorption	H_{surf}	H_{Mg}	H_{MgTi}	H_{Ti}	Absorption	H_{surf}	H_{Mg}	H_{MgTi}	H_{Ti}
$Ti_{24}Mg_{32}H_{112-16}$	1.15	1.56	1.45	1.60	$Ti_{24}Mg_{32}H_{0+16}$	0.09	0.48	−1.10	−1.21
$Ti_{24}Mg_{32}H_{96-32}$	—	0.38	1.40	1.49	$Ti_{24}Mg_{32}H_{32+16}$	−0.43	−0.19	−1.39	—
$Ti_{24}Mg_{32}H_{64-32}$	—	—	1.30	1.38	$Ti_{24}Mg_{32}H_{64+16}$	−0.31	−0.36	—	—
$Ti_{24}Mg_{32}H_{32-32}$	—	—	—	1.10	$Ti_{24}Mg_{32}H_{96+16}$	−1.11	—	—	—

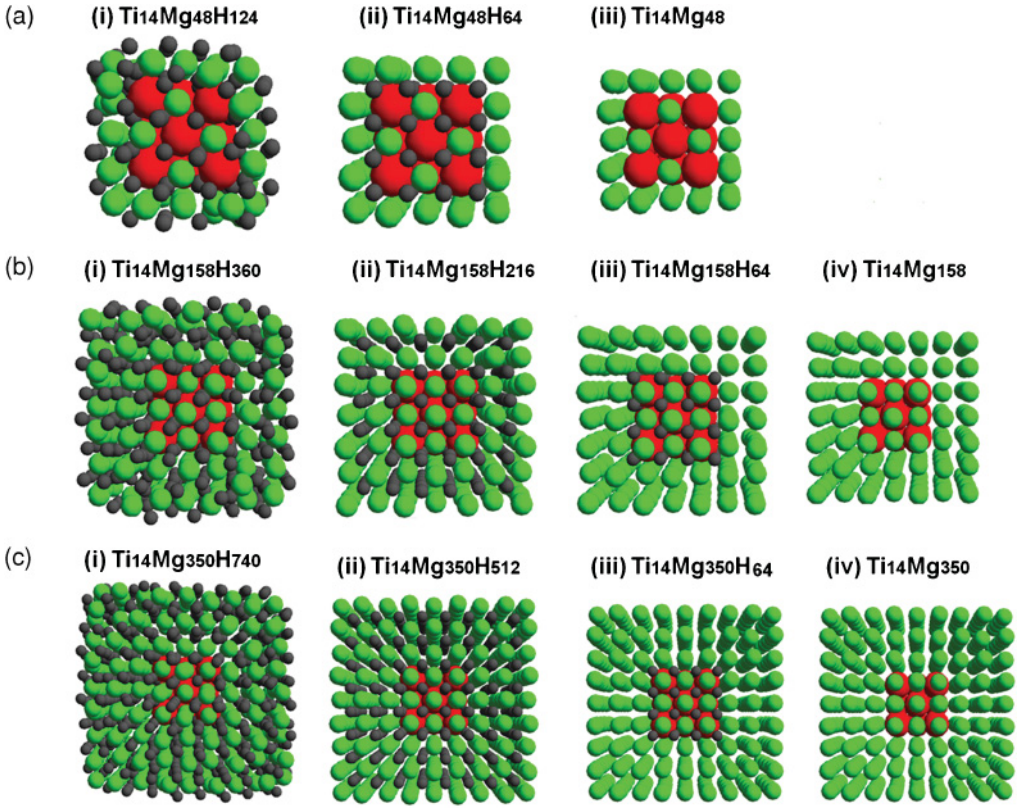

FIG. 3. (Color online) Optimized 3D Ti(core)/Mg(shell) alloys and their fully and partially hydrogenated hydrides involved in the (de)hydrogenation processes. For each Ti/Mg composite, the structures from the left-hand side to the right-hand side indicate the dehydrogenation process.

(0.36 eV/H_2) is very low and after the desorption of H_{surf} and H_{Mg}. Because of the strong Ti-H bonding, the desorption energies of H_{MgTi} and H_{Ti} are always larger than the rutile MgH_2 (0.65 eV/H_2). To save computational time, we combined the desorption of H_{MgTi} with H_{Ti} and only the average desorption of the two was calculated.

Comparing the three hydrides, one can notice the particle size dependence of the hydrogen thermodynamics. On the one hand, the average dehydrogenation energies of all the hydrogen atoms are decreasing with increasing size of the Mg layer, i.e., from 1.22, 0.97, and 0.91 eV/H_2 for $Ti_{24}Mg_{16}H_{80}$, $Ti_{24}Mg_{32}H_{112}$, and $Ti_{24}Mg_{48}H_{144}$, respectively. This can be explained as follows: The larger the population of the Mg-related sites, and the smaller the average hydrogen desorption energy. On the other hand, the desorption energy of H_{surf} increases with increasing Mg layer thickness, from 0.95 eV/H_2 for $Ti_{24}Mg_{16}H_{80}$, to 1.15 eV/H_2 for $Ti_{24}Mg_{32}H_{112}$, to 1.42 eV/H_2 for $Ti_{24}Mg_{48}H_{144}$. The reason for the unexpectedly high desorption energies of H_{surf} and the size dependence will be explained together with the 3D Ti(core)/Mg(shell) structure in Sec. III B 2.

It is worth noting that, for $Ti_{24}Mg_{32}H_{112}$ and $Ti_{24}Mg_{48}H_{144}$, the desorption energies of H_{Mg} (0.38 and 0.36 eV/H_2) are much lower than that of bulk rutile MgH_2 (0.65 eV/H_2). The desorption energy of H_{Mg} is low because the H_{Mg} always occupy the tetrahedral sites in the partially dehydrogenated fluorite type hydrides [see Figs. 2(b)(ii) and 2(c)(ii)]. This is favorable for hydrogen storage application. However, the population of these destabilized hydrogen atoms (H_{Mg}) is low: 1.7 wt % for $Ti_{24}Mg_{32}H_{112}$ and 2.7 wt % for $Ti_{24}Mg_{48}H_{144}$. To obtain a larger population of H_{Mg}, we extend the 2D Mg/Ti/Mg sandwich structure to a 3D Ti(core)/Mg(shell) structure in the next section.

TABLE II. Stepwise and average dehydrogenation energies (in eV/H_2) of three Mg/Ti/Mg sandwich hydrides with different particle sizes and compositions. The hydrogenation energies are not shown as they are identical to the dehydrogenation energy apart from the sign change.

Fig. 2 Mg/Ti/Mg sandwich	H_{surf}	H_{Mg}	H_{MgTi}+H_{Ti}	Average
(a) $Ti_{24}Mg_{16}H_{80}$	0.95	—	1.29	1.22
(b) $Ti_{24}Mg_{32}H_{112}$	1.15	0.38	1.31	0.97
(c) $Ti_{24}Mg_{48}H_{144}$	1.42	0.36	1.33	0.91

B. Ti(core)/Mg(shell) structure

Because the same hydrogen locations can be found in the 2D and 3D structures, we assume that the adsorption sites of H_{surf}, and absorption and desorption sequences found in the 2D structure, also apply for the 3D Ti(core)/Mg(shell) structure. However, it should be emphasized at this point that in the 2D structure, the Mg surfaces are infinitely extended two dimensionally. When hydrogen adsorbs on the Mg surface with a ratio of H/M = 1, an overall ratio of H/M = 2 can always

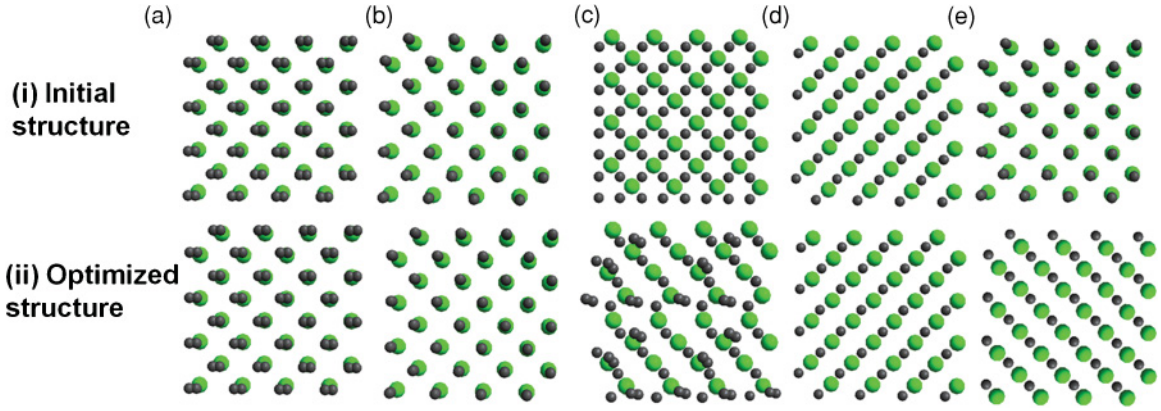

FIG. 4. (Color online) Top view of H_{surf} on a Mg/Ti/Mg sandwich structure [$Ti_{24}Mg_{32}H_x$ in Fig. 2(b), only the top layer of Mg atoms is shown]. The initial and optimized structures are shown as hydrogen dimer adsorption at top sites parallel (a) and perpendicular (b) to the Mg surface with coverage of H/M (surface Mg) = 2, hydrogen atom adsorption at short bridge sites with a coverage of H/M = 2 (c) and H/M = 1 (d), and hydrogen atom adsorption at top site with coverage of H/M = 1 (e).

be obtained. However, for the Ti(core)/Mg(shell) structure slightly different situations were observed. During optimization, the hydrogen atoms adsorbed on the crystallographic facets were indeed stabilized at short bridge (sb) sites, whereas hydrogen atoms on the edges migrated from the sb to the long bridge (lb) sites. The number of sb and lb sites depend highly on the configuration of the core-shell alloy. For instance, 36 (24sb + 12lb), 144 (108sb + 36lb), and 228 (192sb + 36lb) sites are available for hydrogen atoms on the surfaces of $Ti_{14}Mg_{48}$, $Ti_{14}Mg_{158}$, and $Ti_{14}Mg_{350}$ (see Fig. 3), respectively. Together with H_{Mg}, H_{MgTi}, and H_{Ti}, the fully hydrogenated hydrides are $Ti_{14}Mg_{48}H_{124}$, $Ti_{14}Mg_{158}H_{360}$, and $Ti_{14}Mg_{350}H_{740}$, i.e., H/M = 2 or slightly larger than 2. Four single-point calculations with a concentration of $Ti_{14}Mg_{158}H_{352}$ (where eight hydrogen atoms of each type were taken out from $Ti_{14}Mg_{158}H_{360}$) were calculated. The results show the same desorption sequence with what was predicted for the 2D sandwich structure. Therefore, we are confident that the 3D (de)hydrogenation process is similar to that of the 2D structure.

1. The stepwise dehydrogenation energies

The average and stepwise dehydrogenation energies were calculated in the same manner as for the 2D structure. As one can see in Table III, the trends found for the energies in the 2D structure are reproduced: The desorption energies of H_{surf} are very high (except that of $Ti_{14}Mg_{48}H_{124}$); after the desorption of H_{surf}, the desorption energies of H_{Mg} become lower than that of bulk MgH_2; the desorption of $H_{MgTi} + H_{Ti}$ become more difficult due to the strong Ti-H bondings. It is worth noting that for $Ti_{14}Mg_{158}H_{360}$ and $Ti_{14}Mg_{350}H_{740}$, the desorption energies of H_{Mg} (0.39 and 0.27 eV/H_2) are much lower than that of the rutile MgH_2 (0.65 eV/H_2). They are within the desired thermodynamics range and even lower than the lowest H_{Mg} desorption energy of 0.44 eV/H_2 predicted for the MgH_2/TiH_2 multilayers.[31] The desorption energy of H_{Mg} is low because the H_{Mg} atoms always occupy the tetrahedral sites in the partially dehydrogenated hydrides [shown in Figs. 3(b)(ii), and 3(c)(ii)]. This is favorable for hydrogen storage applications.

Comparing the three hydrides, one can again notice the same size dependence of the energies to that of the 2D structure. On the one hand, the average dehydrogenation energies of all hydrogen atoms are decreasing with increasing size of the Mg shell, i.e., 0.80, 0.68, and 0.65 eV/H_2 for $Ti_{14}Mg_{48}H_{124}$, $Ti_{14}Mg_{158}H_{360}$, and $Ti_{14}Mg_{350}H_{740}$, respectively. On the other hand, the desorption energy of H_{surf} increases with increasing size of the Mg shell, from 0.59 eV/H_2 for $Ti_{14}Mg_{48}H_{124}$, to 1.11 eV/H_2 for $Ti_{14}Mg_{158}H_{360}$, to 1.42 eV/H_2 for $Ti_{14}Mg_{350}H_{740}$. The reason for the unexpectedly high values and the size dependence of the desorption energies of H_{surf} will be explained by comparing the structures of the fully and partially hydrogenated hydrides in Sec. III B 2.

2. Structures

To explain the trend found in the dehydrogenation energies of H_{surf} in both 2D and 3D structures, Figs. 2 and 3 should be referred. As one can see, for the fully hydrogenated hydrides, the H_{surf} atoms do not occupy the perfect short bridge site. The hydrogen atoms at the subsurface are also dislocated from perfect tetrehedral sites. These distortions are similar with the deformations which were found in the Mg/Ti multilayers, where with the increasing Mg thickness the fluorite structure tends to change into rutile.[31] For instance, approximately half of the H_{Mg} atoms are closely bonded to H_{surf}. These atoms are ~0.2–0.4 Å closer to the surface Mg than the other half, which are less affected by H_{surf}. This effect extends from one layer to another through the H-H bonding, i.e., from the subsurface of the Mg layer to the Mg/Ti interface. It becomes minor for H_{MgTi} and H_{Ti} atoms as they are stabilized by the strong Ti-H

TABLE III. Stepwise and average dehydrogenation energies (in eV/H_2) of the Ti(core)/Mg(shell) structure.

Fig. 3 Ti(core)/Mg(shell)	H_{surf}	H_{Mg}	$H_{MgTi} + H_{Ti}$	Average
(a) $Ti_{14}Mg_{48}H_{124}$	0.59	—	0.95	0.80
(b) $Ti_{14}Mg_{158}H_{360}$	1.11	0.39	0.90	0.68
(c) $Ti_{14}Mg_{350}H_{740}$	1.42	0.27	0.80	0.65

bonding. Therefore, the structural deformations depend on the size of the Mg layer: The thicker the layer, the more H_{Mg} atoms dislocated by H_{surf}. The structural deformation is direct evidence that H_{Mg} atoms are stabilized upon forming the H-H bonding by the absorption of H_{surf}. This also explains why H_{Mg} becomes unstable upon the desorption of H_{surf} in Sec. III A 2.

However, after the desorption of H_{surf} from the Mg surface, H_{Mg} atoms will relocate at the tetrahedral sites (see Figs. 2 and 3). A well-defined fcc structure is formed again. The fcc symmetry can be preserved in the continuing dehydrogenation process. The desorption energies of H_{surf} were calculated by comparing the energies of the fully hydrogenated and partially hydrogenated hydrides. In this case, they consist of the energy cost of the breaking of the Mg-H_{surf} bond and the energy difference of the Mg-H_{Mg} bonding between the fully and partially hydrogenated hydrides. The latter closely relates to the population of H_{Mg}. Thus the thicker the Mg layer, the more H_{Mg} is stabilized in the fully hydrogenated hydrides, and the larger the H_{surf} desorption energy.

3. *Oversaturation of the Ti(core)/Mg(shell) structure*

The hydrogen storage capacities in nanosized materials can vary from their corresponding bulk materials.[35,43] For instance, Kobayashi *et al.*[43] reported that the capacity of the Pd-Pt nanoparticles with a Pt content of 8–21 at. % was higher than that of pure Pd nanoparticles. The amount of hydrogen absorption is controllable by altering the alloy compositions of Pd and Pt. Wagemans *et al.*[35] predicted that small MgH_2 particles (smaller than $Mg_{15}H_{30}$) have the potential to take up 10%–15% extra hydrogen. They proposed these extra hydrogen atoms are less strongly adsorbed onto the surface of the cluster than the hydrogen absorbed within the cluster. The above results suggest oversaturation of the surface metal.

To verify the potential extra hydrogen in the present nanosized Ti(core)/Mg(shell) alloys, an oversaturation of the $Ti_{14}Mg_{158}$ alloy has been studied. Figure 5(a) shows the initial structure of $Ti_{14}Mg_{158}H_{512}$ (H/M = 2.98), i.e., the fluorite structure with hydrogen terminations. As shown in Fig. 5(b), during the geometric optimization the hydrogen atoms on the Mg surface (H_{surf}) did not dramatically distort the structure of the alloy, but formed different types of hydrogen species. They can be classified as the hydrogen dimer (H-H), hydrogen trimer (H-H-H), hydrogen atoms on facets (H_{face}), and hydrogen atoms at vertices (H_{ver} and H_{ver2}). Except for the hydrogen atoms on the Mg shell surface, the other ones occupy different tetrahedral sites within the Mg shell (H_{Mg}), at the Ti/Mg interface (H_{MgTi}), and within the Ti core (H_{Ti}).

To study the hydrogen bonding properties, the partial density of states (PDOS) of all types of hydrogen atoms in $Ti_{14}Mg_{158}H_{512}$ have been calculated [see Fig. 5(c)]. In the PDOS plot, a sharp peak ~−7.5 eV can be found for the hydrogen dimer. The extremely localized density clearly indicates that no chemical bonds are formed between hydrogen molecules and the alloy. In fact, the hydrogen molecules are "pushed" out of the Mg surface with distances of 2.42 Å (facets) and 2.36 Å (edges), respectively. At vertices, each Mg atom is surrounded by one H_{vera} and three H_{verb}. The H_{vera} is very close to the Mg with a distance of 1.71 Å, whereas the other three H_{verb} are further with a distance of 1.90 Å.

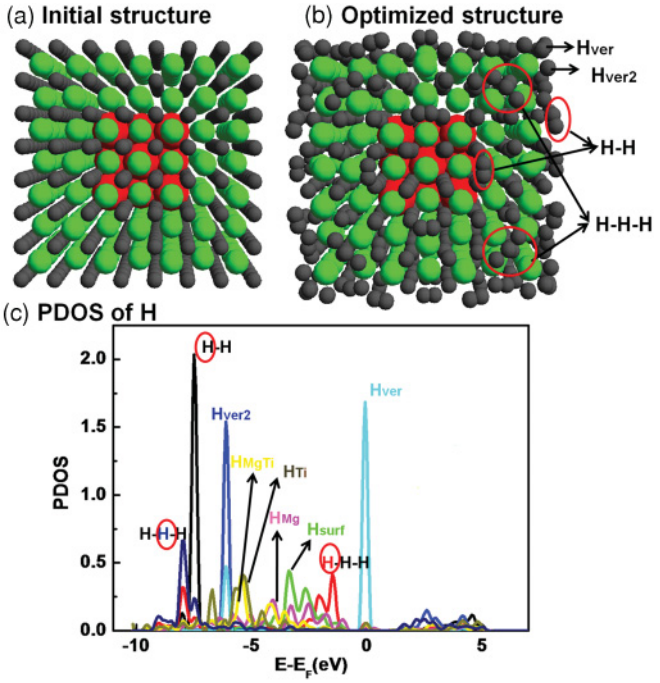

FIG. 5. (Color online) (a) Initial, (b) optimized structure of $Ti_{14}Mg_{158}H_{512}$, and (c) partial density of states (PDOS) of different types of hydrogen atoms found in (b). H-H (hydrogen dimer), H-H-H (hydrogen trimer), H_{ver} and H_{ver2} (hydrogen atoms on the vertexes), and H_{face} (hydrogen atoms on the faces) are different types of hydrogen atoms at the Mg surface (H_{surf}).

The overlap of PDOS of H_{ver} and H_{ver2} ~−6 eV suggests relatively strong bonding between H_{ver} (light blue) and H_{ver2} (dark blue). Moreover, the sharp main peaks of these two indicate barely any bonds formed with the alloys. A similar overlap of the PDOS can be found for the hydrogen trimer but with relatively broader main peaks than the dimer. This indicates that the chemical bonding is mainly localized within the trimer and hardly between the alloy and the trimer. From the structural and electronic analyses above, we conclude that the nonbonding or weak bonding of the hydrogen (trimer, dimer, and the ones on the vertexes) with the Mg surface is a direct consequence of the artificial oversaturation of the alloy. The $Ti_{14}Mg_{158}H_{512}$ (H/M = 2.98) is not a stable hydride. This agrees with the conclusion drawn for the Mg/Ti/Mg sandwich structure in Sec. III A 1.

4. *Reversible capacity*

According to the calculated energies in Secs. III A 3 and III B 1, the very stable H_{surf}, H_{MgTi}, and H_{Ti} prohibits the Mg/Ti/Mg sandwich and Ti(core)/Mg(shell) structures from being used for hydrogen storage materials. However, if one refers to the hydrogenation and dehydrogenation processes in Figs. 2 and 3, one can notice the adsorption of H_{surf} and the desorption of $H_{MgTi} + H_{Ti}$ are the last steps in the hydrogenation and dehydrogenation reactions, respectively. Therefore, partial hydrogenation without absorption of H_{surf} and partial dehydrogenation without the desorption of $H_{MgTi} + H_{Ti}$ would preserve the fluorite symmetry of the core-shell structure and only H_{Mg} with desirable thermodynamic. Partial operation

means that only H_{Mg} will be reversible in the hydrogen cycles. Such reversible hydrogen capacities are estimated to be reasonable high: 3.3 and 4.8 wt % for $Ti_{14}Mg_{158}H_{360}$ and $Ti_{14}Mg_{350}H_{740}$, respectively. They are much higher than the reversible capacity of 1.4 wt % in the Mg/Ti multilayers with a H_{Mg} desorption energy of 0.44 eV/H_2,[31] and also higher than the ones predicted in the Mg/Ti/Mg sandwich structures in Sec. III A 3 (1.7 and 2.7 wt %).

IV. CONCLUSIONS

Hydrogen storage properties of nanosized 2D Mg/Ti/Mg sandwich and 3D Ti(core)/Mg(shell) hydrides have been studied using large-scale DFT calulations. For both structures, four types of hydrogen atoms can be distinguished in the Ti(core)/Mg(shell) hydrides: H_{surf}, H_{Mg}, H_{MgTi}, and H_{Ti}. For the hydrogenation reaction, the hydrogen absorption in the alloys is in the order of H_{Ti}, H_{MgTi}, H_{Mg}, and H_{surf}. For the dehydrogenation reaction, the hydrogen desorption is in the reverse order. The desorption energies of H_{surf} are calculated to be high. The reason is the structural transformation from fluorite to a deformed fluorite structure upon the adsorption of H_{surf}. In other words, the absorption of H_{surf} induces dislocation of H_{Mg} and stabilizes the hydrides. This stabilization effect increases with increasing thickness of the Mg layer. Due to the well-preserved fluorite structure of the partially hydrogenated hydrides, the desorption energies of H_{Mg} are significantly lower than that of bulk MgH_2. This is favorable for hydrogen storage applications. But the further desorption of H_{MgTi} and H_{Ti} is more difficult than that of bulk MgH_2 due to the strong Ti-H bonding. Furthermore, oversaturation of the 3D Ti(core)/Mg(shell) structures is studied. Both the geometric and electronic structure analyses show that the oversaturation of the structure is not stable.

Based on the observed thermodynamic properties, partial hydrogenation without the adsorption of H_{surf} and partial dehydrogenation without the desorption of H_{MgTi} and H_{MgTi} is proposed to preserve the fluorite structure of the hydride with desired thermodynamics. However, this leads to a reduction of the reversible hydrogen capacity. The reversible hydrogen capacity (H_{Mg}) of the Mg/Ti/Mg sandwich structures are low: 1.7 wt % for $Ti_{24}Mg_{32}H_{112}$ and 2.7 wt % for $Ti_{24}Mg_{48}H_{144}$. Those of the Ti(core)/Mg(shell) structures are estimated to be reasonable high: 3.3 and 4.8 wt % for $Ti_{14}Mg_{158}H_{360}$ and $Ti_{14}Mg_{350}H_{740}$, respectively. Our results indicate that the nanosized Ti(core)/Mg(shell) hydrides are very promising hydrogen storage materials with favorable thermodynamics and reasonable hydrogen capacity.

[1] L. Schlapbach and A. Züttel, Nature (London) **414**, 353 (2001).
[2] J. F. Stampfer, C. E. Holley, and J. F. Suttle, J. Am. Chem. Soc. **82**, 3504 (1960).
[3] W. Grochala and P. P. Edwards, Chem. Rev. **104**, 1283 (2004).
[4] B. Bogdanović, K. Bohmhammel, B. Christ, A. Reiser, K. Schlichte, R. Vehlen, and U. Wolf, J. Alloys Compd. **282**, 84 (1999).
[5] B. Bogdanović, Int. J. Hydrogen Energy **9**, 937 (1984).
[6] M. Y. Song, D. R. Mumm, S. N. Kwon, S. H. Hong, and J. S. Bae, J. Alloys Compd. **416**, 239 (2006).
[7] G. Barkhordarian, T. Klassen, and R. Bormann, J. Phys. Chem. B **110**, 11020 (2006).
[8] T. Vegge, L. S. Hedegaard-Jensen, J. Bonde, T. R. Munter, and J. K. Nørskov, J. Alloys Compd. **386**, 1 (2005).
[9] A. J. Du, S. C. Smith, X. D. Yao, and G. Q. Lu, J. Phys. Chem. B **110**, 21747 (2006).
[10] W. P. Kalisvaart, P. Vermeulen, O. Lyedovskykh, D. Danilov, and P. H. L. Notten, J. Alloys Compd. **446**, 648 (2007).
[11] W. P. Kalisvaart, H. J. Wondergem, A. F. Bakker, and P. H. L. Notten, J. Mater. Res. **22**, 1640 (2007).
[12] W. P. Kalisvaart, M. Latroche, F. Cuevas, and P. H. L. Notten, J. Solid State Chem. **181**, 1141 (2008).
[13] S. Srinivasan, P. C. M. M. Magusin, W. P. Kalisvaart, P. H. L. Notten, F. Cuevas, M. Latroche, and R. A. van Santen, Phys. Rev. B **81**, 054107 (2010).
[14] W. P. Kalisvaart and P. H. L. Notten, J. Mater. Res. **23**, 2179 (2008).
[15] R. A. H. Niessen and P. H. L. Notten, Electrochem. Solid-State Lett. **8**, A534 (2005).
[16] K. Nobuhara, H. Kasai, W. A. Di, and H. Nakanishi, Surf. Sci. **566-568**, 703 (2004).
[17] X. D. Yao, C. Z. Wu, A. J. Du, G. Q. Lu, H. M. Cheng, S. C. Smith, J. Zou, and Y. H. He, J. Phys. Chem. B **110**, 11697 (2006).
[18] P. Vermeulen, R. A. H. Niessen, D. M. Borsa, B. Dam, R. Griessen, and P. H. L. Notten, Electrochem. Solid-State Lett. **9**, A520 (2006).
[19] P. H. L. Notten, M. Ouwerkerk, H. van Hal, D. Beelen, W. Keur, J. Zhou, and H. Feil, J. Power Sources **129**, 45 (2004).
[20] P. Vermeulen, R. A. H. Niessen, and P. H. L. Notten, Electrochem. Commun. **8**, 27 (2006).
[21] P. Vermeulen, P. C. J. Graat, H. J. Wondergem, and P. H. L. Notten, Int. J. Hydrogen Energy **33**, 5646 (2008).
[22] D. M. Borsa, R. Gremaud, A. Baldi, H. Schreuders, J. H. Rector, B. Kooi, P. Vermeulen, P. H. L. Notten, B. Dam, and R. Griessen, Phys. Rev. B **75**, 205408 (2007).
[23] G. Liang, J. Huot, S. Boily, A. V. Neste, and R. Schulz, J. Alloys Compd. **291**, 295 (1999); **292**, 247 (1999); **282**, 286 (1999).
[24] B. Zahiri, C. T. Harrower, B. Shalchi-Amirkhiz, and D. Mitlin, Appl. Phys. Lett. **95**, 103114 (2009).
[25] X. Tan, C. T. Harrower, B. Shalchi-Amirkhiz, and D. Mitlin, Int. J. Hydrogen Energy. **34**, 7741 (2009).
[26] J. Lu, Y. Choi, Z. Z. Fang, H. Y. Sohn, and E. Rönnebro, J. Am. Chem. Soc. **131**, 15843 (2009); **132**, 6616 (2010).
[27] A. Baldi, M. Gonzalez-Silveira, V. Palmisano, B. Dam, and R. Griessen, Phys. Rev. Lett. **102**, 226102 (2009).
[28] A. Baldi, G. K. Pálsson, M. Gonzalez-Silveira, H. Schreuders, M. Slaman, J. H. Rector, G. Krishnan, B. J. Kooi, G. S. Walker, M. W. Fay, B. Hjörvarsson, R. J. Wijngaarden, B. Dam, and R. Griessen, Phys. Rev. B **81**, 224203 (2010).
[29] B. R. Pauw, W. P. Kalisvaart, S. X. Tao, M. T. M. Koper, A. P. J. Jansen, and P. H. L. Notten, Acta Mater. **56**, 2948 (2008).
[30] S. Er, D. Tiwari, G. A. de Wijs, and G. Brocks, Phys. Rev. B **79**, 024105 (2009).
[31] S. X. Tao, P. H. L. Notten, R. A. van Santen, and A. P. J. Jansen, Phys. Rev. B **82**, 125448 (2010).

[32]K. C. Kim, B. Dai, J. K. Johnson, and D. S. Sholl, Nanotechnology **20**, 204001 (2009).
[33]J. J. Liang and W. C. Kung, J. Phys. Chem. B **109**, 17837 (2005).
[34]V. Berube, G. Radtke, M. Dresselhaus, and G. Chen, Int. J. Hydrogen Res. **31**, 637 (2007).
[35]R. Wagemans, J. H. van Lenthe, P. E. de Jong, A. J. van Dillen, and K. P. de Jong, J. Am. Chem. Soc. **127**, 16675 (2005).
[36]J. Liang, Appl. Phys. A: Mater. Sci. Process. **80**, 173 (2005).
[37]S. Cheung, W.-Q. Deng, A. C. T. van Duin, and W. A. Goddard, J. Phys. Chem. A **109**, 851 (2005).
[38]G. Kresse and J. Furthmüller, Phys. Rev. B **54**, 11169 (1996).
[39]G. Kresse and J. Furthmüller, Comput. Mater. Sci. **6**, 15 (1996).
[40]G. Kresse and D. Joubert, Phys. Rev. B **59**, 1758 (1999).
[41]J. P. Perdew, Physica B **172**, 1 (1991).
[42]H. J. Monkhorst and J. D. Pack, Phys. Rev. B **13**, 5188 (1976).
[43]H. Kobayashi, M. Yamauchi, H. Kitagawa, Y. Kubota, K. Kato, and M. Takata, J. Am. Chem. Soc. **132**, 5576 (2010).